

## Research paper

## Loading and delivery of sertraline using inorganic micro and mesoporous materials

Carla D. Nunes <sup>a</sup>, Pedro D. Vaz <sup>a</sup>, Ana C. Fernandes <sup>b</sup>, Paula Ferreira <sup>c</sup>,  
Carlos C. Romão <sup>b</sup>, Maria José Calhorda <sup>a,\*</sup>

<sup>a</sup> Departamento de Química e Bioquímica, Universidade de Lisboa, Lisboa, Portugal

<sup>b</sup> Instituto de Tecnologia Química e Biológica, Universidade Nova de Lisboa, Oeiras, Portugal

<sup>c</sup> Departamento de Engenharia Cerâmica e do Vidro, Universidade de Aveiro, Aveiro, Portugal

Received 21 June 2006; accepted in revised form 22 November 2006

Available online 5 December 2006

---

### Abstract

Sertraline hydrochloride (designated as sertraline from now on) is an antidepressive drug with unpleasant effects in the gastric tract. Therefore, improved means of delivery allowing for a more controlled and efficient release were looked for. Two different porous materials, montmorillonite-K10 and MCM-41, were chosen as hosts. The drug was intercalated in the interlayer spacing of the clay by cation exchange and was loaded inside the MCM-41 channels by pore volume impregnation means. Spectroscopic evidence (UV/vis, FTIR, powder X-ray diffraction (XRD) and <sup>13</sup>C CP/MAS and <sup>29</sup>Si CP/MAS and MAS solid-state NMR), as well as elemental analysis, complemented by DFT calculations, demonstrated the presence of sertraline in the composite materials. The release processes were monitored under in vitro conditions using a simulated body fluid. The release profile from the clay is fast, indicating that a concentration peak is reached in a short period of time, while the release profile from MCM is slower but lasts longer. These differences are discussed on the basis of different therapeutic indications for both materials.

© 2006 Elsevier B.V. All rights reserved.

**Keywords:** Microporous materials; Mesoporous materials; Sertraline; Drug delivery systems; Controlled release

---

### 1. Introduction

The drug delivery process is of major importance in assuring that a certain molecule will arrive without decomposition or secondary reactions at the right place to perform its task with efficiency. The drug is introduced as part of an inert matrix, from which it should be released in a controlled way and where it should be distributed uniformly. Despite the improvements experienced in the latest years, better delivery systems are still needed. Nanotechnology approaches have been very valuable. Besides polymers, liposomes, cyclodextrins and other matrices used to circumvent this problem, inorganic micro and mesoporous

materials based on clays and silica have also been shown to have adequate, in some cases advantageous characteristics [1–4].

MCM-41 is a one-dimensional material with ordered hexagonal channels running in one direction, which belongs to the M41S family, discovered in 1992 [5,6]. It has been widely studied owing to many attractive features, including a stable mesoporous structure, large surface area (usually >1000 m<sup>2</sup>/g), narrow pore size distribution, and well-defined surface properties, and has proved to be very good for hosting molecules of several sizes, shapes and functionalities. The functionalized materials have been applied in many fields, such as, among others, catalysis, adsorption/sorption, separation, sensing, optically active materials and are making their entry into drug delivery [7–10].

The clays can be described as two-dimensional materials, since they are formed by layers of double hydroxides, and allow the intercalation of other species between them.

---

\* Corresponding author. Departamento de Química e Bioquímica, Faculdade de Ciências, Universidade de Lisboa, Ed. C8, Campo Grande, 1749-016 Lisboa, Portugal. Tel.: +351 217500196; fax: +351 217500088.

E-mail address: [mjc@fc.ul.pt](mailto:mjc@fc.ul.pt) (M.J. Calhorda).

Montmorillonite is a bio-inert clay mineral with fine grain and large interlayer-planar spacing in the (001) plane with a superior capability to intercalate large molecules into this space [11]. The interlayer-space depends much on conditions, becoming more open in basic medium, especially at pH values above 11 [12]. This particular clay has many known applications in a variety of fields, in a similar way to MCM-41 described above [13–15]. It has been shown to exhibit catalytic activity in a wide variety of chemical processes, such as oxidation of olefins and halo-hydrocarbons, hydrocarbon cracking and isomerization [16,17]. This versatility is tuned by the use of mixed-ion systems, where some elements, such as Ga, La, Ce, Fe, Mn or Cr, substitute some of the divalent cations from the lamellar sheets.

In recent years, both materials have started also to be investigated for their capabilities concerning storage and delivery of intercalated substances, such as biologically active drugs, vitamins, amino acids, and mono-oligonucleotides [1–4,12]. Also, the interaction between the drugs and the walls of the materials, within the available space, disrupts the crystalline order of the structure, separating molecules or ions from one another. These “isolated” species, also known as the amorphous form [18], are more easily solubilized by the physiological medium. Besides the higher dissolution rates of the drugs, the use of mesoporous microparticles has also contributed to decrease the pH dependency of drug's behavior [19].

Sertraline is a new antidepressant drug developed along with venlafaxine, fluvoxamine, mirtazapine, fluoxetine, citalopram. It is administered orally and used to treat mental depression, obsessive-compulsive disorder, panic disorder, premenstrual dysphoric disorder, post-traumatic stress disorder, and social anxiety disorder. It is not chemically related to tricyclic, tetracyclic, or other available antidepressant agents and has fewer cardiovascular and anticholinergic adverse effects than these, but it is known for causing adverse secondary effects in the gastric tract [20–23]. The proposed inorganic supports should behave as active antacids, as montmorillonite contains magnesium and aluminium, while MCM-41 has a siliceous matrix, and silicon may exhibit properties similar to those of aluminium. Furthermore the intercalation is considered a new approach to improve drug solubility and even to decrease the ulceration side effects of the drug, as it has been recently described [12,19,24]. Also, the size of the molecule suggests that it may fit either the pores or the intralamellar gallery of the materials.

The composite materials prepared have been characterized by several spectroscopic techniques and their efficiency as drug delivery systems evaluated *in vitro*.

## 2. Experimental section

### 2.1. Materials and methods

Starting materials were obtained from commercial sources and used as received. Sertraline hydrochloride

was obtained from Sigma, and all other reagents, including montmorillonite-K10 (hereafter denoted as **K10**), from Aldrich Chimica. Solvents were dried by standard procedures – CaH<sub>2</sub> (methylene chloride and chloroform) – distilled under nitrogen and kept over 4 Å molecular sieves. Simulated body fluid was prepared following the ionic composition defined for c-SBF according to Oyane et al. [25]. Microanalyses were performed at the Elemental Analysis Service of ITQB. Powder XRD data were collected on a Phillips PW1710 diffractometer using Cu-K $\alpha$  radiation filtered by graphite. TGA studies were performed using a Perkin-Elmer TGA7 thermobalance system at a heating rate of 10 K min<sup>-1</sup> under air. FTIR spectra in transmission or absorbance modes were measured in the range 400–4000 cm<sup>-1</sup> using 2 cm<sup>-1</sup> resolution with a Mattson Satellite FTIR spectrometer using KBr pellets. <sup>1</sup>H and <sup>13</sup>C solution NMR spectra were obtained with a Bruker Avance-400 spectrometer. <sup>29</sup>Si and <sup>13</sup>C solid-state NMR spectra were recorded at 79.49 and 100.62 MHz, respectively, on a (9.4 T) Bruker Avance 400 P spectrometer. <sup>29</sup>Si MAS NMR spectra were recorded with 40° pulses, spinning rates 5.0–5.5 kHz, and 60 s recycle delays. <sup>29</sup>Si CP/MAS NMR spectra were recorded with 5.5  $\mu$ s <sup>1</sup>H 90° pulses, 8 ms contact time, a spinning rate of 4.5 kHz, and 4 s recycle delays. <sup>13</sup>C CP/MAS NMR spectra were recorded with a 4.5  $\mu$ s <sup>1</sup>H 90° pulse, 2 ms contact time, a spinning rate of 8 kHz, and 4 s recycle delays. Chemical shifts are quoted in ppm from TMS. <sup>13</sup>C spectra were also recorded in the solid state at 125.76 MHz on a Bruker Avance 500 spectrometer.

The controlled release tests were carried out suspending the composite materials under continuous stirring at the temperature of 37  $\pm$  0.1 °C in a simulated body fluid (SBF), maintaining a ratio of ml SBF/mg sertraline absorbed equal to 1 and at pH 7.4.

Absorbance measurements were made at regular time intervals at a selected wavelength ( $\lambda_{\text{max}}$  = 275 nm) on a UV-vis Shimadzu spectrometer with a temperature cell and stirring. Absorbance measured values were fitted against a calibration curve based on a Lambert-Beer law.

### 2.2. Preparation of materials and drug loading

The drug loading described below for the two materials was found to be reproducible by  $\pm$ 5%.

#### 2.2.1. MCM-41 (MCM)

This material was synthesized as previously reported from a gel containing cetyltrimethylammonium bromide, and a silicate sodium solution [26]. The surfactant was removed by calcination at 540 °C for 6 h in air. IR (KBr,  $\nu$ , cm<sup>-1</sup>): 3417 (vs, br d), 1631 (m), 1225 (vs), 1082 (vs), 946 (s), 798 (m), 565 (m). <sup>29</sup>Si MAS NMR ( $\delta$  ppm): -94.7 (Q<sup>2</sup>), -103.5 (Q<sup>3</sup>), -109.5 (Q<sup>4</sup>).

#### 2.2.2. Loading in montmorillonite (K10sert)

The mixture of montmorillonite K-10 (1.0 g) and sertraline (500 mg) in dichloromethane (50 mL) was stirred for 3

days at room temperature under a nitrogen atmosphere. After filtration, the solid was dried under *vacuo* during several hours. Elemental analysis found (%): C 7.29, N 0.48, H 0.99. IR (KBr,  $\nu$ ,  $\text{cm}^{-1}$ ): 3630 (s), 3423 (vs, br d), 2947 (w), 2864 (w), 2712 (vw), 1629 (m), 1471 (w), 1402 (vw), 1229 (vs, br d), 1050 (vs, br d), 925 (s, sh), 795 (m).  $^{13}\text{C}$  CP/MAS NMR ( $\delta$  ppm): 19.7, 25.5, 29.7, 44.4, 55.5, 129.5, 140.1, 145.3.  $^{29}\text{Si}$  MAS NMR ( $\delta$  ppm):  $-94.3$  ( $\text{Q}^2$ ),  $-104.0$  ( $\text{Q}^3$ ),  $-111.7$  ( $\text{Q}^4$ ).

### 2.2.3. Loading in MCM-41 (MCMsert)

Prior to the incorporation of sertraline, physisorbed water was removed from calcined MCM-41 by heating at  $180^\circ\text{C}$  in vacuum ( $10^{-2}$  Pa) for 2 h. The mixture of MCM-41 (1.0 g) and sertraline (500 mg) in dichloromethane (50 mL) was stirred for 3 days at room temperature under nitrogen atmosphere. After filtration, the solid was dried under *vacuo* during several hours. Elemental analysis found (%): C 11.44, N 0.70, H 0.84. IR (KBr,  $\nu$ ,  $\text{cm}^{-1}$ ): 3643 (s, sh), 3424 (vs, br d), 2966 (w), 2852 (w), 2717 (vw), 1625 (m), 1474 (w), 1401 (vw), 1235 (vs), 1079 (vs), 965 (s), 809 (m).  $^{13}\text{C}$  CP/MAS NMR ( $\delta$  ppm): 19.7, 24.9, 31.1, 45.0, 57.8, 130.0, 140.7, 145.9.  $^{29}\text{Si}$  MAS NMR ( $\delta$  ppm):  $-92.2$  ( $\text{Q}^2$ ),  $-102.4$  ( $\text{Q}^3$ ),  $-108.9$  ( $\text{Q}^4$ ).

### 2.3. Computational details

DFT [27] calculations were performed on sertraline hydrochloride using the Gaussian 03 program, rev. B.04. [28]. Molecular geometry, based on the published crystallographic structure [29], was fully optimized without any symmetry constraints at the B3LYP [30] level with the 6-31G\* basis set [31] on all atoms. Frequency calculations were performed at the same level to confirm the nature (minimum) of the stationary point determined. NMR chemical shifts were calculated using the GIAO algorithm [32] and referenced to TMS (tetramethylsilane).

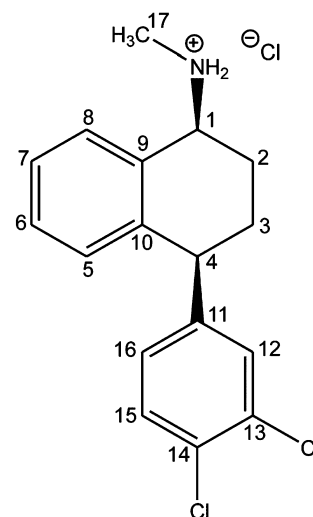
## 3. Results and discussion

### 3.1. Structure and calculations of the drug molecule

Sertraline is isolated as the hydrochloride, *cis*-(1*S*,4*S*)-*N*-methyl-4(3,4-dichlorophenyl)-1,2,3,4-tetrahydro-1-naphthalenamine hydrochloride, and the structure is represented in Scheme 1, with the atom numbering scheme. It acts selectively as an inhibitor of the reuptake of serotonin (5-hydroxytryptamine, 5-HT) (SSRI).

The structure of sertraline hydrochloride, obtained from a single crystal X-ray structure determination, is available [29]. In the crystal, each chloride ion bridges two sertraline cations through hydrogen bonds, forming chains along the crystal. Two sertraline cations bridged by one  $\text{Cl}^-$  are shown in Fig. 1.

DFT calculations were performed on sertraline hydrochloride. The geometry was fully optimized, using DFT calculations (B3LYP/6-31G\* in GAUSSIAN03), without



Scheme 1.

any symmetry constraints, and the vibrational infrared spectrum and the NMR chemical shifts were evaluated. The results were mainly used to assign the experimental spectra of the free compound. The optimized geometry is also given in Fig. 2, with the indication of the approximate dimensions of the optimized molecule.

The geometrical parameters of the sertraline cation compare very well with those from the crystallographic X-ray structure. The same cannot be said about the hydrogen bonds, because the network existent in the solid was not totally considered in the calculations. The chloride is only involved in one  $\text{N-H}\cdots\text{Cl}$  bond, instead of two. This will obviously affect the description. The model will be acceptable for the intended purpose, namely assigning IR and NMR spectra, if the hydrogen bonds are not particularly relevant.

On the other hand, it is expected that sertraline will not remain as a crystal inside the pores of the materials upon loading. Instead, the ionic, hydrogen bonds, and other interactions inside the crystal will be replaced by analogous interaction between the sertraline cation, chloride, etc., and

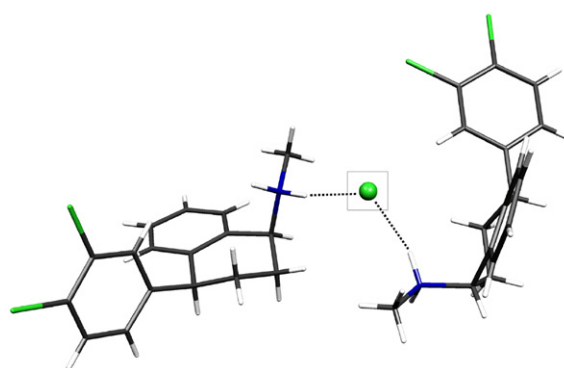


Fig. 1. The basic motif of the hydrogen-bond network in the crystal structure of sertraline hydrochloride.

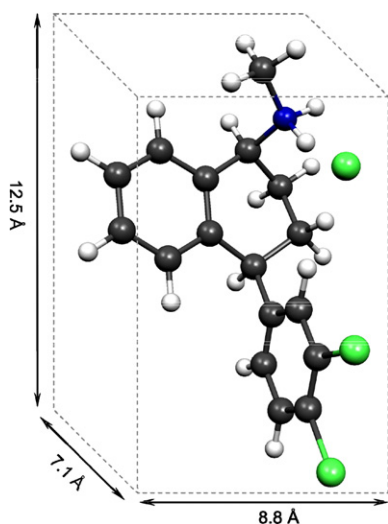


Fig. 2. DFT optimized geometry (B3LYP/6-31G\*) of sertraline hydrochloride.

the walls. The cation will probably be a better model for this amorphous form than the crystal motif.

### 3.2. Characterization of the materials

Sertraline hydrochloride (**sert**) was incorporated in montmorillonite (**K10**) and in MCM-41 (**MCM**), as described in Section 2, affording two composite materials designated as **K10sert** and **MCMsert**.

The FTIR spectra of the host (**K10** and **MCM**) and loaded (**K10sert** and **MCMsert**) materials, as well as the experimental and calculated vibrational spectra of **sert** are collected in Fig. 3.

The spectra of both **K10** and **MCM** host materials are dominated by the  $\nu_{\text{O-H}}$  modes, presenting broad and intense bands at  $3423\text{ cm}^{-1}$  (**K10**) and  $3424\text{ cm}^{-1}$  (**MCM**). These are assigned to hydrogen-bonded hydroxyl groups, whereas bands at  $3630\text{ cm}^{-1}$  (**K10**) and  $3643\text{ cm}^{-1}$  (**MCM**) are indicative of free OH groups of the host matrices. Broad and very intense features in the range  $1000$ –

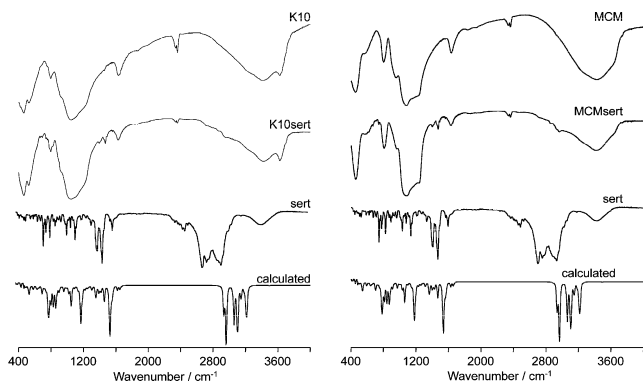


Fig. 3. FTIR of pure sertraline (**sert**), hosts (**K10** and **MCM**), and composite materials (**K10sert** and **MCMsert**). Also shown is the DFT calculated infrared spectrum (not corrected).

$1200\text{ cm}^{-1}$  are also present. These correspond to  $\nu_{\text{Si-O-Si}}$  modes of the siliceous matrix of **MCM** and to  $\nu_{\text{Al-Al-OH}}$ ,  $\nu_{\text{Al-O-Si}}$  and  $\nu_{\text{Si-O-Si}}$  modes of the layers of **K10** clay. In particular, for **K10**, the bands at  $930\text{ cm}^{-1}$  and at  $540\text{ cm}^{-1}$  correspond to the  $\nu_{\text{Al-Al-OH}}$ ,  $\nu_{\text{Al-O-Si}}$  modes, respectively, and are characteristic of the octahedral layer of the clay [33,34].

Although the spectra of the composite materials **MCMsert** and **K10sert** are dominated by the bands of the host material, it is possible to see the presence of **sert** owing to small, but relevant, spectral features that offer a positive identification of the guest. In **K10sert**, a set of three broad and very weak bands in the  $\nu_{\text{C-H}}$  modes region at  $2947\text{ cm}^{-1}$ ,  $2864\text{ cm}^{-1}$ , and  $2712\text{ cm}^{-1}$  indicates that sertraline is present in the interlayer spacing of the host clay, without dramatic structural changes. Also visible is a pair of bands at  $1472\text{ cm}^{-1}$  and  $1402\text{ cm}^{-1}$ , assigned to the C–H bending and C=C stretching modes of the drug molecule. The corresponding wavenumbers in the experimental IR spectrum of pure sertraline are found at  $2934\text{ cm}^{-1}$ ,  $2884\text{ cm}^{-1}$  and  $2698\text{ cm}^{-1}$  (for  $\nu_{\text{C-H}}$  modes) and  $1464\text{ cm}^{-1}$  and  $1402\text{ cm}^{-1}$  (for  $\beta_{\text{C-H}}$  and  $\nu_{\text{C=C}}$  modes). DFT eigenvalues (not corrected) for these vibrational modes are estimated to occur at  $3201\text{ cm}^{-1}$ ,  $3091\text{ cm}^{-1}$  and  $2954\text{ cm}^{-1}$  in what concerns the  $\nu_{\text{C-H}}$  modes and at  $1519\text{ cm}^{-1}$  and  $1451\text{ cm}^{-1}$  for the  $\beta_{\text{C-H}}$  and  $\nu_{\text{C=C}}$  modes. This is in very good agreement with experimental data.

In **MCMsert**, the bands corresponding to the  $\nu_{\text{C-H}}$  modes of loaded sertraline are observed at  $2966\text{ cm}^{-1}$ ,  $2852\text{ cm}^{-1}$  and  $2717\text{ cm}^{-1}$ , while the  $\beta_{\text{C-H}}$  and  $\nu_{\text{C=C}}$  modes are evidenced by the presence of bands at  $1474\text{ cm}^{-1}$  and  $1401\text{ cm}^{-1}$ . The observation of this pattern indicates that the drug was successfully loaded inside the pores of the MCM mesoporous material. The decrease of the shoulder at ca.  $960\text{ cm}^{-1}$  indicates that the Si–OH surface groups of **MCM** are interacting with amino groups of **sert** molecules, as discussed recently by Xia [23]. Comparison between the observed values found for **K10sert** and **MCMsert** shows that some bands are shifted. This situation may be due to the establishment of different types of host–guest interactions (H-bond, ionic or other) between sertraline and **K10** or **MCM**. In both cases this may in fact be related to the different drug release profiles presented by these composite materials, as will be discussed later.

The XRD powder patterns of all host (**K10** and **MCM**) and composite (**K10sert** and **MCMsert**) materials are shown in Fig. 4. For comparison, we added the pattern of pure sertraline and physical mixtures of **sert** and each of the host materials. For the montmorillonite system, most of the characteristic peaks in the two patterns are in the same position, except the characteristic peak indexed to the (001) reflection that is observed at  $2\theta = 8.7^\circ$  for **K10** and is shifted to  $2\theta = 4.7^\circ$  for **K10sert**.

According to Bragg's law, peaks shifting from higher to lower diffraction angles are explained by a  $d$ -spacing increase, which in this case would be from  $10.1\text{ Å}$  to  $18.6\text{ Å}$  upon loading of the drug. Assuming that the



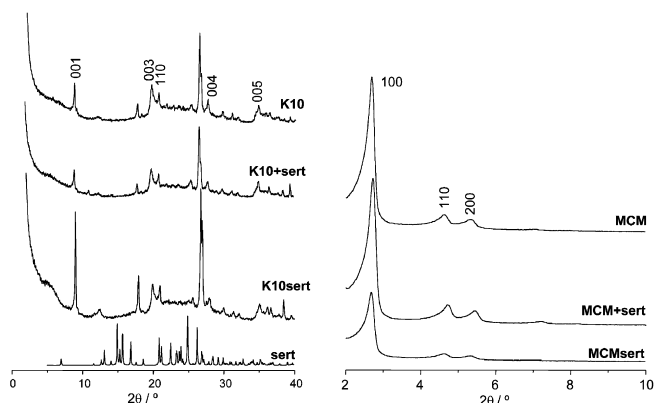
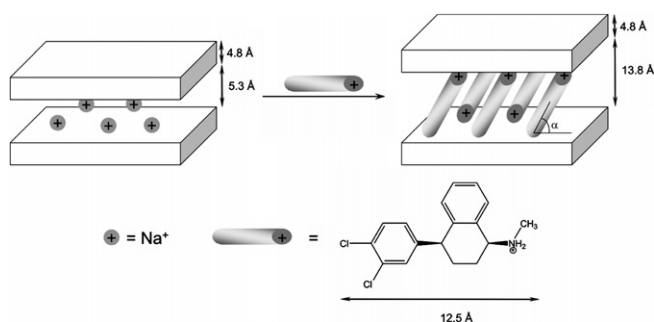


Fig. 4. XRD powder patterns of host (**K10** and **MCM**), **sert**, composite materials (**K10sert** and **MCMsert**), and physical mixtures of **sert** with each support.

alumino-silicate layer is ca. 4.8 Å thick [16], this results in a gallery increase from 5.3 Å to 13.8 Å upon intercalation of the drug. According to DFT calculations (see Fig. 2) the maximum dimension of the sertraline molecule is ca. 12.5 Å. By considering the gallery height to be 13.8 Å, it is possible to estimate the tilt angle of the drug molecules in the interlayer gallery ( $\alpha$  in Scheme 2) as approximately 66°. Taking this value into account, a proposal for the interlayer arrangement of the drug molecules is shown in Scheme 2 (not at scale). This arrangement should be taken with care, as it results from a rough estimation and much more extensive theoretical work would be required to obtain a more accurate value.

Considering now the MCM materials (Fig. 4), three reflections indexed to a hexagonal cell can be observed for the **MCM** powder pattern, the first corresponding to the (100) reflection, the second to (110) and the last to (200) plane. The value of  $d$  for the (100) reflection is 32.6 Å, corresponding to a lattice constant of  $a = 37.6$  Å. The XRD powder pattern of **MCMsert** is quite similar to that of **MCM**, with the reflections of (100), (110) and (200) planes, which indicate retention of the long range hexagonal symmetry. There is a slight attenuation of XRD peak intensities, that should not be interpreted as a loss of crystallinity, but, more likely, to a reduction in



Scheme 2.

the X-ray scattering contrast between the silica wall and the pore filling material [35,36].

The powder XRD profiles of the physical mixtures of both **K10** and **sert**, and **MCM** and **sert** (Fig. 4) of the mixtures differ from those of the composite materials and do not show any differences when compared to the XRD powder patterns of the bulk parent materials. This is expected since mixing does not allow a real inclusion of the guest within either the interlayer spacing of **K10** or of the mesopores of **MCM**.

Fig. 5 shows the TGA analyses to sertraline and all the materials (host and composite) herein discussed. Both **MCM** and **K10** host materials show mass losses until 100 °C corresponding to physisorbed water. After this temperature only a small quantity of mass is still lost by both materials.

The TGA curve of **sert** shows an almost complete mass loss reaching ca. 90% in the 190–340 °C temperature range. This may be ascribed to a severe decomposition of the drug. Afterwards, there are two further mass losses of, respectively, 4% and 7% until the final temperature of 800 °C. Given the first abrupt mass loss, no estimation of how the molecule is degraded can be made.

In what concerns the **K10sert** composite material the loss of physisorbed water is also observed until 200 °C. Afterwards, a two-step mass loss is accomplished by the material corresponding to the gradual decomposition of the sertraline molecule. This mass loss reaches ca. 15%, corresponding to a 0.05 mol% of sertraline, assuming that all this weight loss is due to sertraline. In the case of the **MCMsert** composite material, the same two-step pattern is observed at temperatures above 100 °C and matches that of the **K10sert** material. This two-step weight loss corresponds to ca. 25% and corresponds to 0.07 mol% of sertraline inside the **MCM** pores. These values – 0.05 mol% (**K10sert**) and 0.07 mol% (**MCMsert**) – agree with those from elemental analysis, found to be 0.04 mol% and 0.06 mol%, respectively. The observation that mass losses are observed until ca. 650 °C can be taken as an indication that the drug is mostly inside either the intragallery spacing of **K10** or the mesopores of **MCM** materials.

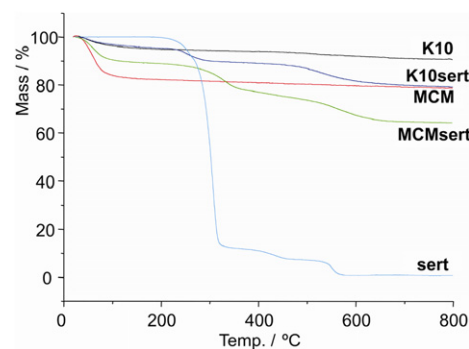


Fig. 5. TGA profiles of bulk **sert** drug and the materials **K10**, **K10sert**, **MCM**, and **MCMsert**.

$^{29}\text{Si}$  NMR spectra of **K10** and **K10sert** are shown in Fig. 6, along with those from **MCM** and **MCMsert**. For the clay samples, three resonances are observed at  $-94.3$  ppm ( $Q^2$ ),  $-104.0$  ppm ( $Q^3$ ) and  $-111.7$  ppm ( $Q^4$ ). The species can be assigned to silicon species where the  $[\text{SiO}_4]^{4-}$  tetrahedra are surrounded, respectively, by two, three or four silicon atoms. The other neighboring atoms can be aluminium or hydrogen. If Al and H are generically represented as X, the species can be represented as:  $Q^2 = (\text{SiO})_2\text{-Si-(OX)}_2$ ,  $Q^3 = (\text{SiO})_3\text{-Si-(OX)}$  and  $Q^4 = (\text{SiO})_4\text{-Si}$  [11]. It is expected that X is essentially aluminium because of the low quality of the  $^{29}\text{Si}$  CP MAS NMR spectra (not shown). In what concerns the **MCM** and **MCMsert** materials, two convoluted resonances are clearly observed at  $-102.4$  ppm and at  $-108.9$  ppm, assigned to  $Q^3$  and  $Q^4$  species, respectively [ $Q^n = \text{SiO}_{4-n}\text{Si(OH)}_n$ ]. The signal assigned to the  $Q^2$  species has a very weak intensity and appears at  $-92.2$  ppm.

These results show that loading of sertraline either in the interlayer spacing of **K10** clay or inside the pores of **MCM** did not affect to a great extent the structure of the host materials.

$^{13}\text{C}$  NMR of pure sertraline (observed in solution and DFT calculated) and the solid-state CP MAS of **K10sert** and **MCMsert** appear in Fig. 7.

The calculated chemical shifts compare very well with the experimental data from the spectrum of pure sertraline. These resonances at 22.9, 27.6, 44.9 and 56.3 ppm are thus assigned to the  $\text{C}_2$ ,  $\text{C}_3$ ,  $\text{C}_4$  and  $\text{C}_1$  aliphatic carbon atoms of the fused ring (Scheme 1), and the methyl group ( $\text{C}_{17}$ ) appears at 29.5 ppm. The assignment of the resonances of the aromatic carbon atoms is not as straightforward, with the exception of  $\text{C}_{10}$  and  $\text{C}_{11}$  that appear at higher chemical shifts.

The solid-state spectra from composite materials **K10sert** and **MCMsert** exhibit lower resolution, as expected. Nevertheless, by comparison with the liquid  $^{13}\text{C}$  NMR spectrum of pure sertraline it is possible to identify the broad and intense resonance at 130 ppm as being due to the aromatic nuclei of the drug molecule. Also, other features at  $\delta = 60$  ppm and 50 ppm and a broad signal at  $\delta = 25.0$  ppm can be assigned to the remaining aliphatic cyclic carbon atoms. The methyl group of sertraline is

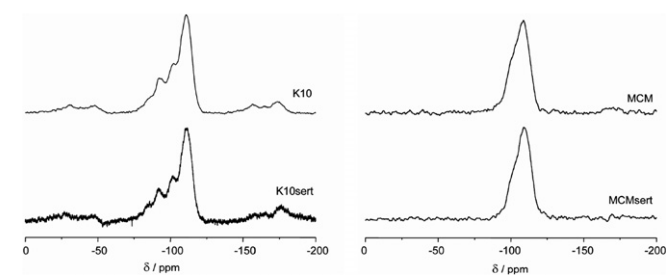


Fig. 6.  $^{29}\text{Si}$  MAS spectra of host materials (**K10**, **MCM**) and composite materials (**K10sert** and **MCMsert**).

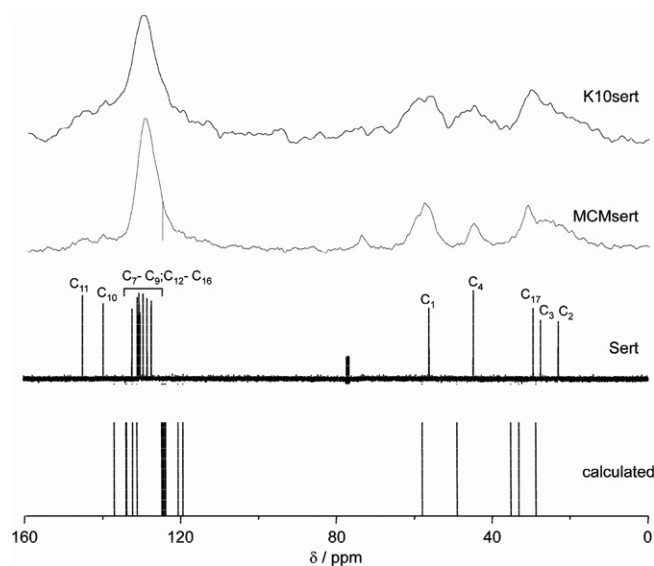


Fig. 7.  $^{13}\text{C}$  NMR solid-state spectra of host materials (**K10**, **MCM**) and composite materials (**K10sert** and **MCMsert**). Also shown is the liquid  $^{13}\text{C}$  NMR spectrum of sertraline together with DFT calculated chemical shifts. Assignments are based on the DFT calculated results.

observed at  $\delta = 35$  ppm. These observations indicate the successful loading of the drug inside the hosts.

### 3.3. Drug release profiles

Typical drug release profiles for the different types of investigated materials are plotted in Fig. 8 (the same profiles containing error bars can be found in [Electronic Supplementary Material – Figure ES11](#)). The controlled release tests were carried out suspending the composite materials under continuous stirring at the temperature of  $37 \pm 0.1$  °C in a simulated body fluid (SBF), maintaining a ratio of ml SBF/mg sertraline absorbed equal to 1 and at pH 7.4. The chosen ratio comprehends a value well below the estimated thermodynamic solubility (4.24 mg/ml at

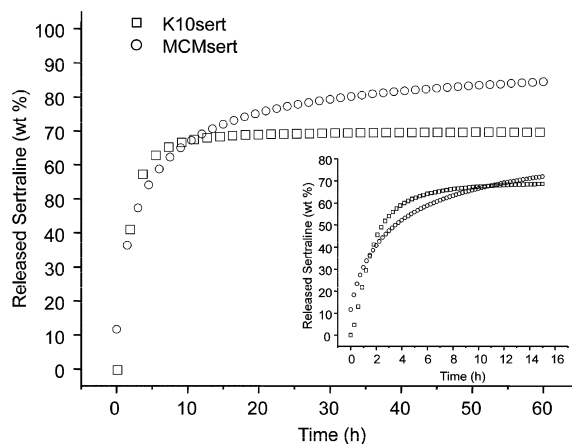


Fig. 8. Drug release profiles of both composite materials at 37 °C in a simulated body fluid. The inset shows the release profile on the first 15 h stressing the different initial release profiles.

pH 6.05), and with a population of the protonated species of the drug of ca. 97% at pH 7.4 [37]. The measurements were made at regular time intervals using UV/vis spectroscopy at a wavelength of 275 nm. The measured values were then fitted against a calibration curve determined with the pure sertraline dissolved in SBF (Lambert–Beer law). Since the ratio of ml SBF/mg sertraline absorbed was initially set to 1, the 100% mark in Fig. 8 corresponds to the complete release of **sert** drug. This means that in a complete release test a concentration of 1 mg **sert**/ml SBF should be measured.

The results presented in Fig. 8 show that after a period of 60 h none of the samples (**MCMsert** and **K10sert**) had completely released the drug. However, longer times did not help to release higher quantities, as reported recently in a study concerning gentamicin delivery [24]. This fact is more significant in the release profile of **K10sert**, where the release percentage stayed below 70–80%. This fact may be explained by the existence of electrostatic interactions between the protonated amino groups of the sertraline cations and the anionic groups from the layers of the **K10** clay [3,12]. In the case of the **MCMsert** sample, the interaction between host–guest species is mainly by means of hydrogen bonding between the guest molecule and the silanol groups at the surface of the host material. Therefore, the weaker host–guest interactions should contribute to a more extensive release of the guest in this case. A similar situation has already been described previously by Vallet-Regi and co-workers, while studying MCM-41 loaded with ibuprofen [2].

The release rate of sertraline from the host matrices was found to be higher for **K10sert** than for **MCMsert**. In particular, the initial delivery rates (calculated in the first 2 h of release) were calculated to be  $0.7 \text{ mg h}^{-1}$  for **K10sert** and  $0.4 \text{ mg h}^{-1}$  for **MCMsert**. The calculated rate constants were determined by fitting the absorbance vs. time data to Eq. (1):

$$W_t = W_\infty (1 - e^{-kt})$$

where  $W_t$  and  $W_\infty$  are the quantities of sertraline at time  $t$  and at the end of reaction, respectively, and  $k$  represents the calculated rate. A simpler linear fit of the initial values (to  $t = 4 \text{ h}$  in the inset of Fig. 8) provided roughly the same results. **K10sert** has a higher initial capacity of delivering the loading to the biological medium and therefore is more effective in a situation where a rapid peak concentration of the drug is needed. By contrast, **MCMsert** is somewhat slower (rate ca. 40% slower than found for **K10sert**) in the initial delivery, but achieves a constant delivery rate. This can be relevant for situations of long-term treatment, where a delivery of the drug under continuous rate is expected.

The fast initial delivery rate has been observed in other related studies and explained by the authors as part of the drug being adsorbed outside the material or lying at the entrance of the pores [24].

#### 4. Conclusions

Sertraline, an antidepressive drug, was loaded in montmorillonite, a microporous clay, and MCM-41, a mesoporous material with a hexagonal array of the channels. The strong bands from the hosts observed in the FTIR spectra of both composite materials obtained only left a feeble evidence of the presence of the guest. Solid-state  $^{13}\text{C}$  NMR results, on the other hand, reveal signals characteristic of sertraline, thus showing that the integrity of the guest is maintained upon loading. DFT calculations allowed the assignment of NMR chemical shifts and vibrational frequencies. Powder XRD patterns show an increase in the d-spacing when going from **K10** to **K10sert**, required to accommodate sertraline in the interlayer space, and a decrease of the peaks' intensity in **MCMsert** consistent with mesoscopic order kept when sertraline occupies the pores of **MCM**. These results and solid-state  $^{29}\text{Si}$  NMR data confirm that the structures of both host materials are only slightly perturbed by the introduction of sertraline.

The composite materials behave differently concerning drug release. **K10sert** has faster release kinetics, but **MCMsert** delivers higher quantities of sertraline at a slower rate. Therefore, each material can be more appropriate depending on requirements. A faster response, as presented by **K10sert**, is relevant for situations where high seric concentrations must be achieved in a short period of time, whereas the slower though continued response of **MCMsert** is more suitable for long-term treatment situations thus reducing the need of dose administration. Finally, none of the drug-loaded materials was able to deliver the total amount of drug. This may arise from strong interactions between the drug molecules and the surfaces of the materials, which are not overcome by interaction with the solvent (low solubility).

#### Acknowledgements

CDN (SFRH/BPD/14512/2003) and PDV (SFRH/BPD/14903/2004) thank FCT for research grants. We thank FCT for financial support (POCI/QUIM/58925/2004 and POCTI/QUI/44654/2002). Conceição Almeida is acknowledged for the elemental analyses at the ITQB.

#### Appendix A. Supplementary data

Supplementary data associated with this article can be found, in the online version, at [doi:10.1016/j.ejpb.2006.11.023](https://doi.org/10.1016/j.ejpb.2006.11.023).

#### References

- [1] M. Vallet-Regí, J.C. Doadrio, A.L. Doadrio, I. Izquierdo-Barba, J. Pérez-Pariente, Hexagonal ordered mesoporous material as a matrix for the controlled release of amoxicillin, *Solid State Ionics* 172 (2004) 435–439.

- [2] B. Muñoz, A. Rámila, J. Pérez-Pariente, I. Díaz, M. Vallet-Regí, MCM-41 organic modification as drug delivery rate regulator, *Chem. Mater.* 15 (2003) 500–503.
- [3] T. Kollár, I. Pálkó, Z. Kónya, I. Kiricsi, Intercalating amino acid guests into montmorillonite host, *J. Mol. Struct.* 651–653 (2003) 335–340.
- [4] G. Cavallaro, P. Pierro, F.S. Palumbo, F. Testa, L. Pasqua, R. Aiello, Drug delivery devices based on mesoporous silicate, *Drug Delivery* 11 (2004) 41–46.
- [5] C.T. Kresge, M.E. Leonowicz, W.J. Roth, J.C. Vartuli, J.S. Beck, Ordered mesoporous molecular sieves synthesized by a liquid-crystal template mechanism, *Nature* 359 (1992) 710–712.
- [6] J.S. Beck, J.C. Vartuli, W.J. Roth, M.E. Leonowicz, C.T. Kresge, K.D. Schmitt, C.T.W. Chu, D.H. Olson, E.W. Sheppard, S.B. McCullen, J.B. Higgins, J.L. Schlenker, A new family of mesoporous molecular sieves prepared with liquid crystal templates, *J. Am. Chem. Soc.* 114 (1992) 10834–10843.
- [7] D.M. Ford, E.E. Simanek, D.F. Shantz, Engineering nanospaces: ordered mesoporous silicas as model substrates for building complex hybrid materials, *Nanotechnology* 16 (2005) S458–S475.
- [8] H.D. Zhang, Y.H. Sun, K.Q. Ye, P. Zhang, Y. Wang, Oxygen sensing materials based on mesoporous silica MCM-41 and Pt(II)–porphyrin complexes, *J. Mater. Chem.* 15 (2005) 3181–3186.
- [9] F.J. Brieler, P. Grundmann, M. Froba, L.M. Chen, P.J. Klar, W. Heimbrot, H.A.K. von Nidda, T. Kurz, A. Loidl, Comparison of the magnetic and optical properties of wide-gap (II,Mn)VI nanostructures confined in mesoporous silica, *Eur. J. Inorg. Chem.* (2005) 3597–3611.
- [10] M. Jia, A. Seifert, M. Berger, H. Giegengack, S. Schulze, W.R. Thiel, Hybrid mesoporous materials with a uniform ligand distribution: synthesis, characterization, and application in epoxidation catalysis, *Chem. Mater.* 16 (2004) 877–882.
- [11] K.-W. Park, O.-Y. Kwon, Interlamellar silylation of Montmorillonite with 3-Aminopropyltriethoxysilane, *Bull. Kor. Chem. Soc.* 25 (2004) 965–968.
- [12] F.H. Lin, Y.H. Lee, C.H. Jian, J.-M. Wong, M.-J. Shieh, C.-Y. Wang, A study of purified montmorillonite intercalated with 5-fluorouracil as drug carrier, *Biomaterials* 23 (2002) 1981–1987.
- [13] M. Pospíšil, P. Čapková, D. Měřínská, Z. Maláč, J. Šimoník, Structure analysis of montmorillonite intercalated with cetylpyridinium and cethylmethylammonium: molecular simulations and XRD analysis, *J. Coll. Int. Sci.* 236 (2001) 127–131.
- [14] A. Clearfield, Role of ion exchange in solid-state chemistry, *Chem. Rev.* 88 (1988) 125–148.
- [15] C. Zhou, X. Li, Z. Ge, Q. Li, B. Tong, Synthesis and acid catalysis of nanoporous silica/alumina-clay composites, *Catal. Today* 93–95 (2004) 607–613.
- [16] K. Ohtsuka, Preparation and properties of two-dimensional microporous pillared interlayered solids, *Chem. Mater.* 9 (1997) 2039–2050.
- [17] A. Gil, L.M. Gandia, M.A. Vicente, Recent advances in the synthesis and catalytic applications of pillared clays, *Catal. Rev. Sci. Eng.* 42 (2000) 145–212.
- [18] B.C. Hancock, M. Parks, What is the true solubility advantage for amorphous pharmaceuticals? *Pharm. Res.* 17 (4) (2000) 397–403.
- [19] J. Salonen, L. Laitinen, A.M. Kaukonen, J. Tuura, M. Björkqvist, T. Heikkilä, K. Väälä-Heikkilä, J. Hirvonen, V.-P. Lehto, Mesoporous silicon microparticles for oral drug delivery: loading and release of five model drugs, *J. Control. Release* 108 (2005) 362–374.
- [20] D. Chen, S. Jiang, Y. Chen, Y. Hu, HPLC determination of sertraline in bulk drug, tablets and capsules using hydroxypropyl- $\beta$ -cyclodextrin as mobile phase additive, *J. Pharm. Biomed. Anal.* 34 (2004) 239–245.
- [21] F. Chen, M.B. Larsen, C. Sánchez, O. Wiborg, The *S*-enantiomer of *R,S*-citalopram, increases inhibitor binding to the human serotonin transporter by an allosteric mechanism. Comparison with other serotonin transporter inhibitors, *Eur. Neuropsychopharmacol.* 15 (2005) 193–198.
- [22] M. Vaswani, F.K. Linda, S. Ramesh, Role of selective serotonin reuptake inhibitors in psychiatric disorders: a comprehensive review, *Prog. Neuropsychopharmacol. Biol. Psychiatry* 27 (2003) 85–102.
- [23] J.W. Trauger, A. Jiang, B.A. Stearns, P.V. Lograsso, Kinetics of Allopregnanolone formation catalyzed by human  $3\alpha$ -hydroxysteroid dehydrogenase type III (AKR1C2), *Biochemistry* 41 (2002) 13451–13459.
- [24] W. Xia, J. Chang, Well-ordered mesoporous bioactive glasses (MBG): a promising bioactive drug delivery system, *J. Control. Release* 110 (2006) 522–530.
- [25] A. Oyane, H.-M. Kim, T. Furuya, T. Kokubo, T. Miyazaki, T. Nakamura, Preparation and assessment of revised simulated body fluids, *J. Biomed. Mater. Res.* 65A (2003) 188–195.
- [26] C.D. Nunes, A.A. Valente, M. Pillinger, A.C. Fernandes, C.C. Romão, J. Rocha, I.S. Gonçalves, MCM-41 functionalized with bipyridyl groups and its use as a support for oxomolybdenum(VI) catalysts, *J. Mater. Chem.* 12 (2002) 1735–1742.
- [27] R.G. Parr, W. Yang, *Density Functional Theory of Atoms and Molecules*, University Press, Oxford, New York, 1989.
- [28] M.J. Frisch, G.W. Trucks, H.B. Schlegel, G.E. Scuseria, M.A. Robb, J.R. Cheeseman, J.A. Montgomery, Jr., T. Vreven, K.N. Kudin, J.C. Burant, J.M. Millam, S.S. Iyengar, J. Tomasi, V. Barone, B. Mennucci, M. Cossi, G. Scalmani, N. Rega, G.A. Petersson, H. Nakatsuji, M. Hada, M. Ehara, K. Toyota, R. Fukuda, J. Hasegawa, M. Ishida, T. Nakajima, Y. Honda, O. Kitao, H. Nakai, M. Klene, X. Li, J.E. Knox, H.P. Hratchian, J.B. Cross, V. Bakken, C. Adamo, J. Jaramillo, R. Gomperts, R.E. Stratmann, O. Yazyev, A.J. Austin, R. Cammi, C. Pomelli, J.W. Ochterski, P.Y. Ayala, K. Morokuma, G.A. Voth, P. Salvador, J.J. Dannenberg, V.G. Zakrzewski, S. Dapprich, A.D. Daniels, M.C. Strain, O. Farkas, D.K. Malick, A.D. Rabuck, K. Raghavachari, J.B. Foresman, J.V. Ortiz, Q. Cui, A.G. Baboul, S. Clifford, J. Cioslowski, B.B. Stefanov, G. Liu, A. Liashenko, P. Piskorz, I. Komaromi, R.L. Martin, D.J. Fox, T. Keith, M.A. Al-Laham, C.Y. Peng, A. Nanayakkara, M. Challacombe, P.M.W. Gill, B. Johnson, W. Chen, M.W. Wong, C. Gonzalez, J.A. Pople, *Gaussian 03*, Revision B.01, Gaussian, Inc.: Wallingford CT, 2004.
- [29] F. Caruso, A. Besmer, M. Rossi, The absolute configuration of sertraline (Zoloft) hydrochloride, *Acta. Crystallogr. C55* (1999) 1712–1714.
- [30] (a) A.D. Becke, Density-functional thermochemistry. III. The role of exact exchange, *J. Chem. Phys.* 98 (1993) 5648–5652;  
(b) B. Miehlich, A. Savin, H. Stoll, H. Preuss, Results obtained with the correlation energy density functionals of Becke and Lee, Yang and Parr, *Chem. Phys. Lett.* 157 (1989) 200–206;  
(c) C. Lee, W. Yang, G. Parr, Development of the Colle-Salvetti correlation-energy formula into a functional of the electron density, *Phys. Rev. B* 37 (1988) 785–789.
- [31] (a) A.D. McClean, G.S. Chandler, Contracted Gaussian basis sets for molecular calculations. I. Second row atoms,  $Z = 11$ –18, *J. Chem. Phys.* 72 (1980) 5639–5648;  
(b) R. Krishnan, J.S. Binkley, R. Seeger, J.A. Pople, Self-consistent molecular orbital methods. XX. A basis set for correlated wave functions, *J. Chem. Phys.* 72 (1980) 650–654;  
(c) A.J.H. Wachters, Gaussian basis set for molecular wavefunctions containing third-row atoms, *J. Chem. Phys.* 52 (1970) 1033–1036;  
(d) P.J. Hay, Gaussian basis sets for molecular calculations. The representation of 3d orbitals in transition-metal atoms, *J. Chem. Phys.* 66 (1977) 4377–4384;  
(e) K. Raghavachari, G.W. Trucks, Highly correlated systems. Excitation energies of first row transition metals Sc–Cu, *J. Chem. Phys.* 91 (1989) 1062–1065;  
(f) R.C. Binning, L.A. Curtiss, Extension of Gaussian-2 theory to molecules containing third-row atoms Ga–Kr, *J. Chem. Phys.* 103 (1995) 6104–6113;  
(g) M.P. McGrath, L. Radom, Extension of Gaussian-1 (G1) theory to bromine-containing molecules, *J. Chem. Phys.* 94 (1991) 511–516.
- [32] (a) K. Wolinski, J.F. Hilton, P. Pulay, Efficient implementation of the gauge-independent atomic orbital method for NMR chemical shift



- calculations, *J. Am. Chem. Soc.* 112 (1990) 8251–8260;
- (b) K. Wolinski, A.J. Sadlej, Self-consistent perturbation-theory – open-shell states in perturbation-dependent non-orthogonal basis-sets, *Mol. Phys.* 41 (1980) 1419–1430;
- (c) R. Ditchfield, Self-consistent perturbation-theory of diamagnetism. I. Gauge-invariant LCAO method for NMR chemical-shifts, *Mol. Phys.* 27 (1974) 789–807;
- (d) R. McWeeny, Perturbation theory for the Fock–Dirac density matrix, *Phys. Rev.* 126 (1962) 1028–1034.
- [33] P. Komadel, J. Bujdak, J. Madejova, V. Sucha, F. Elsass, Effect of non-swelling layers on the dissolution of reduced-charge montmorillonite in hydrochloric acid, *Clay Miner.* 31 (1996) 333–345.
- [34] A. Nasser, M. Gal, Z. Gerstl, U. Mingelrn, S. Yariv, Adsorption ofalachlor by montmorillonites, *J. Thermal Anal.* 50 (1997) 257–268.
- [35] B. Marler, U. Oberhagemann, S. Voltmann, H. Gies, Influence of the sorbate type on the XRD peak intensities of loaded MCM-41, *Micro. Mater.* 6 (1996) 375–383.
- [36] W. Hammond, E. Prouzet, S.D. Mahanti, T.J. Pinnavaia, Structure factor for the periodic walls of mesoporous MCM-41 molecular sieves, *Microporous Mesoporous Mater.* 27 (1999) 19–25.
- [37] K. Deák, K. Takács-Novák, K. Tihanyi, B. Noszál, Physico-chemical profiling of antidepressive sertraline. Solubility, ionization, liophilicity, *Med. Chem.* 2 (2006) 385–389.